Journal of ELECTRONIC MATERIALS, Vol. 45, No. 7, 2016
DOI: 10.1007/s11664-016-4477-6

Effect of A Site and Oxygen Vacancies on the Structural and Electronic Properties of Lead-Free $KTa_{0.5}Nb_{0.5}O_3$ Crystal

WENLONG YANG,[1] LI WANG,[1] JIAQI LIN,[1,2,4] XIAOKANG LI,[1] HANJIANG XIU,[1] and YANQING SHEN[3]

1.—Department of Applied Science, Harbin University of Science and Technology, Harbin 150001, People's Republic of China. 2.—Key Laboratory of Engineering Dielectrics and Its Application, Ministry of Education, Harbin University of Science and Technology, Harbin 150080, People's Republic of China. 3.—Department of Physics, Harbin Institute of Technology, Harbin 150001, People's Republic of China. 4.—e-mail: ljqi405@163.com

The structural and electronic properties of lead-free potassium tantalite niobate $KTa_{0.5}Nb_{0.5}O_3$ (KTN) with A site vacancies V_K^0, V_K^{1-} and oxygen vacancies V_O^0, V_O^{2+}, were investigated by first-principles calculations, which indicated that A site vacancies V_K^0 are likely to form in the KTN compared with V_K^{1-}, and oxygen vacancies V_O^{2+} are likely to form compared with V_O^0 in the KTN according to the investigation of formation energy. The results show that K and O vacancies have significant influence on the atomic interactions of the atoms and the electronic performance of the materials. And Ta atoms are more easily influenced by the K and O vacancies than the Nb atoms from the atomic displacements in KTN with K and O vacancies. The investigation of density of state indicates that the compensation of electrons in KTN with vacancies make the hybridization become stronger among Ta d, Nb d and O p orbitals. Besides, Mulliken population of all the Ta and Nb atoms in KTN with charged vacancies are influenced by complement electrons. The strength of the Nb-O bond is stronger than Ta-O based on the changes of bond lengths and Mulliken population.

Key words: $KTa_{0.5}Nb_{0.5}O_3$, first principle, vacancies, electronic properties

INTRODUCTION

Defects are inevitably introduced into materials in the preparation process and often play an important role in controlling the properties of materials, such as optical absorption edge, electrical performances, and thermoelectric energy conversion.[1–4] Usually, the defects are very difficult to control precisely in materials by conventional experimental instruments. The atoms and defects could be modulated by advanced preparation techniques, such as molecular beam epitaxy (MBE) and chemical vapor deposition (CVD), but the experimental condition is relatively strict and expensive.[5,6] However, theoretical simulation is an efficient method to investigate the effects caused by the change of microstructure, and to expose the relations between the internal structures and the electrical, optical properties.[7]

In recent years, the promising perovskite materials have been widely investigated, and many achievements have been obtained on the ABO_3 perovskite materials vacancies through the theoretical research methods, such as optical properties of oxygen vacancy in $KNbO_3$,[8] electronic structure of oxygen vacancy in $SrTiO_3$,[9] formation of vacancies in potassium sodium niobate,[10] structural and electronic properties of oxygen vacancy in lead-free KTN,[11] surface rumpling calculation in ABO_3 materials,[12] intrinsic point defects in oxides of the perovskite family,[13] the magnetization induced by vacancies in $SrTiO_3$,[14] the nature of atomic relaxation around oxygen-vacancy defects in $PbTiO_3$,[15] stain effects in reactivity of $LaCoO_3$ with oxygen vacancy,[16] native defects and lanthanum impurities

(Received January 23, 2015; accepted March 19, 2016; published online April 11, 2016)

in $NaTaO_3$,[17] and oxygen vacancy in perovskite oxides.[18,19]

Potassium tantalite niobate crystal ($KTa_{1-x}Nb_xO_3$, KTN) is a solid solution of $KTaO_3$ and $KNbO_3$, and it is one of the most promising materials for the electro-optical, holographic, ferroelectric and piezoelectric applications.[20–22] It is known that the vacancies are formed inevitably because of the high volatility of the K elements in the growth of the KTN crystal and O vacancies as intrinsic point defects in oxides of the perovskite family, which both would significantly influence the electrical and optical properties of the materials. However, the study about K vacancy in the KTN materials has not been well explored. The O and K vacancies will occur simultaneously in the experiment. In order to overcome high volatility of the K element and undesirable qualitites of KTN materials caused by O vacancy in the experiment, excess K_2CO_3 was usually added in the stoichiometric mixtures to obtain K enriched ceramics, and controlling O_2 atmospheric pressure to compensate O vacancy.[23]

In order to investigate the properties of $KTa_{0.5}Nb_{0.5}O_3$ with K vacancy, based on the first-principles, a series of calculations had been carried out. The effects of K vacancy on the geometry structures and electronic characteristics of KTN were studied in this work. As a comparison, the properties of O vacancy in KTN had been explored at the same time.

COMPUTATIONAL DETAILS

In this paper, the first-principles calculations were performed with the plane-wave pseudopotential total energy code in the framework of density functional theory (DFT).[24] The ultrasoft pseudopotentials (USPs) were employed in the local density approximation (LDA) for the exchange and correlation energies.[25]

In the KTN materials, Ta ions and Nb ions are located randomly on the B sites. Although the disordered solid structure can not be simulated in the computer, the theoretical simulation of ordered KTN could also provide some information about the intrinsic interaction of materials. The ordered KTN with perovskite structure, which has B site cations that ordered along the [111] direction, is the most stable.[26] For the simulation of the vacancy of KTN, geometry optimizations on the $2 \times 2 \times 2$ ordered KTN supercells were performed to relax the shape of the cell and the atomic positions of KTN crystals. The parameters used in the calculations are as follows: the maximum cutoff energy of the plane waves was taken as 380 eV and the $4 \times 4 \times 4$ Monkhorst–Pack mesh was used to sample the Brillouin zone. In addition, all calculated results were tested for convergences with respect to the number of K-points and the cutoff energy of the plane waves.

In order to compare the different cases, a series of calculations have been performed. The supercell of pure KTN, the potassium vacancy with 0 charged (V_K^0), −1 charged (V_K^{1-}) of KTN and the oxygen vacancy (V_O^0) with 0 charged, +2 charged (V_O^{2+}) are shown in Fig. 1a–c, respectively. The vacancy atoms are marked with arrows, as shown in Fig. 1b and c.

RESULTS AND DISCUSSIONS

Geometry Structure and Energetic Stability

After geometry optimization, the stable ground states were achieved. The optimized structures of pure KTN, KTN with V_K^0 and V_K^{1-} belong to the cubic phase, *Pm*3*m* group, and the optimized structures of KTN with V_O^0 and V_O^{2+} belong to the tetragonal phase, *P*4*mm* group. The computational data of the structure parameters are presented in Table I. It can be seen that there are significant changes in the structures by the introduction of the K and O vacancies. And the calculated lattice parameters are similar to experimental data, Wang et al. had reported lattice parameters a = 4.00289 Å, 4.00251 Å, and 3.99279 Å corresponding to three different raw materials ratios: Ta_2O_5:Nb_2O_5 (mol) = 0.65:0.35, 0.55:0.45, and 0.35:0.65, respectively.[27] Compared with the pure KTN, the lattice parameters and the volume of KTN with V_K^0 become smaller caused by the K vacancy. However, the lattice parameters of KTN with V_K^{1-} become larger when an electron was compensated for the K vacancy as shown in Table I. In order to investigate the stability of the V_K^0 and V_K^{1-} in KTN, the formation energy of the defects were calculated.

In terms of the formation energy of KTN, the formation energy of q charged vacancies in KTN can be calculated from the total energies of supercells using the standard formalism as follows[28–30]:

$$\Delta E_f^V = E_{tot}^V - E_{tot} + \mu_v + q(\varepsilon_{VBM} + E_f) \qquad (1)$$

where E_{tot}^V and E_{tot} are the total energies of the supercells with vacancy and supercells perfect, respectively. μ_v is the chemical potential of certain atoms removed from the perfect supercell. E_f is the Fermi level measured from the valence band maximum (ε_{VBM}), and Fermi level is set at zero energy in the LDA calculation.

The formation energy of pure KTN, KTN with K and O vacancies were calculated according to the express formula, and the results are presented in Table I. The formation energy of KTN with V_K^{1-} is larger than that of V_K^0, which means that the K vacancy with 0 charged is likely to form in the KTN compared with −1 charged K vacancy. Whereas, the formation energy of KTN with V_O^0 is larger than that of V_O^{2+}, which indicates that the +2 charged O vacancy is more stable than V_O^0 in the KTN. It can be seen that not only the types of the element but

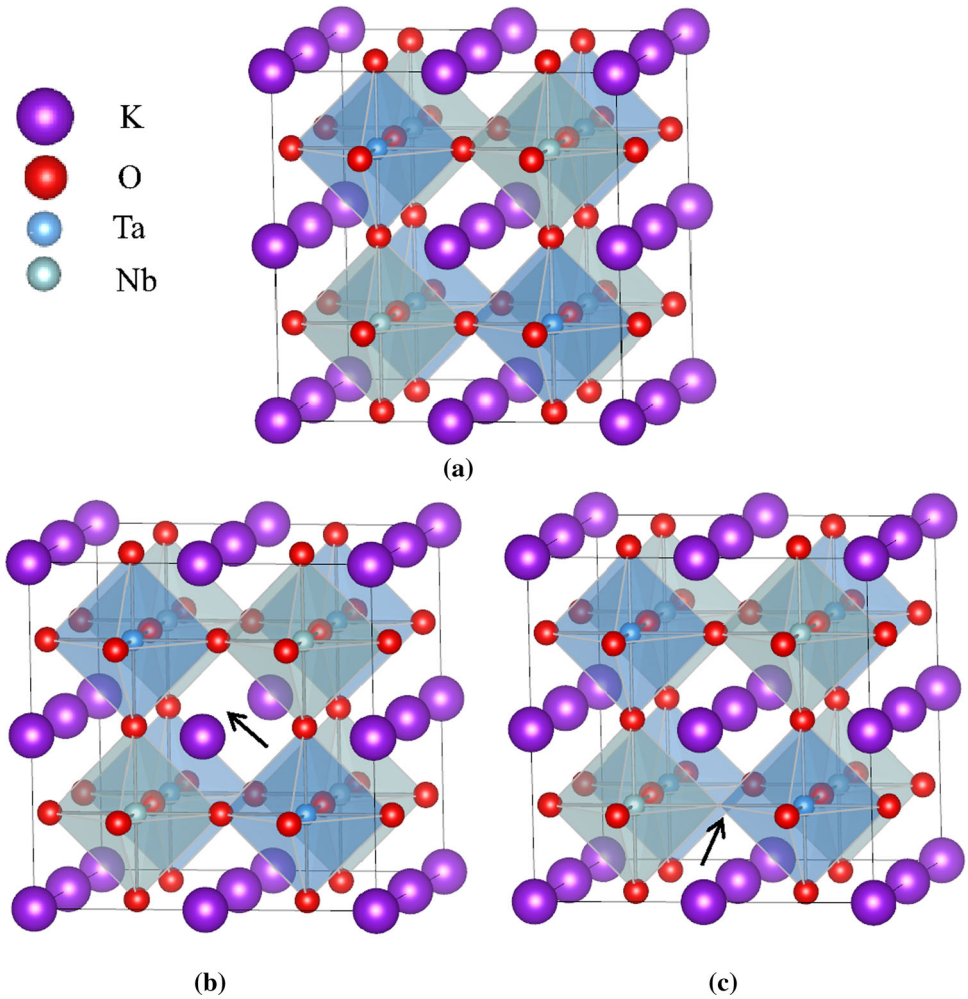

Fig. 1. Supercell of (a) pure KTN, (b) KTN with potassium vacancy, and (c) KTN with oxygen vacancy (Color figure online).

Table I. Structure parameters, energy gap E_{gap} and formation energies of [111] pure KTN, KTN with V_K^0, KTN with V_K^{1-}, KTN with V_O^0 and KTN with V_O^{2+}

Parameter	KTN	V_K^0	V_K^{1-}	V_O^0	V_O^{2+}
a (Å)	7.9813	7.9706	8.0209	8.0027	7.9016
b (Å)	7.9813	7.9706	8.0209	7.9737	7.8359
c (Å)	7.9813	7.9705	8.0210	7.9737	7.8358
V (Å^3)	508.4180	506.3653	516.0365	508.8132	485.1618
E_{gap} (eV)	1.578	1.671	1.569	1.701	1.565
E^f (eV)	0	7	13	−42	−62

also the charge compensation formation contributes to the formation ability and stability of defects in the materials. Therefore, we can predict based on the stability that A site vacancies V_K^0 are likely to form in the KTN compared with V_K^{1-} and oxygen vacancies V_O^{2+} are likely to form compared with V_O^0 in the KTN during the practical process of preparation. And some experiments show the O_2, N_2 or K_2O atmospheres are the effective methods for controlling vacancies.[23,31,32] The high saturated vapor pressure is the fatal issue for K element volatilization and the formation of the K vacancy, and the K_2O atmosphere has been confirmed to be an effective way for the K vacancy controlling, while the O atmosphere is an admitted way to restrain the O defect, and the N_2 atmosphere is conductive to the formation of the O vacancy. There are three methods for charge compensation of the vacancies. First, the charge compensation could be achieved by the A-site and B-site cation ions substitution.[17,33] For

example, the A-site K vacancies V_K^{1-} will be formed when a K atom is removed and the V_K^0 will appear when an A-site K atom is replaced by a bivalent cation, such as Ca^{2+}, Ba^{2+} and Mg^{2+} etc. Whereas the O vacancy is a double donor, a V_K^0 vacancy would be formed though B-site substitution by two quadrivalent cations or one trivalent cation, such as Zr^{4+}, Ti^{4+}, Sr^{4+}, Ce^{4+} and Ce^{3+}, and La^{3+}.[17,33] Second, the charge injection, which is usually used for the traps investigation of dielectric materials, is another effective method for charge compensation.[34] Because V_K^{1-} and V_O^{2+} vacancies are the negative and positive centers in the KTN crystal, they will become the capture centers for the positive hole and the electron, respectively. In addition, the charged vacancies could adsorb the charged particles in the air for the charge compensation. Therefore, the controlling of charge compensation contributes to the improvement of properties.

The atomic displacements of K, Ta, Nb and O atoms closest to K vacancy and O vacancy were presented in Table II. Obvious differences can be seen from the atomic displacements closed to K and O defects. For K vacancy, the nearest O atoms will move away from the vacancy while the nearest Ta atoms will be closer when a K atom is removed away. For O vacancy, the other O atoms will move closer to the O vacancy and the Ta, Nb and K atoms will move away from the O vacancy when one O atom is removed. The displacements of Nb atoms change inconspicuously compared with the Ta atoms no matter which vacancy occurs. Thus it can be seen that Ta atoms are more easily influenced by the K and O vacancies than the Nb atoms.

The results can be explained by the Coulomb interaction. It is well known that the KTN crystal has the perovskite structure, and the oxygen octahedron is the basic frame, which is distributed in the periodic K atoms lattice. The Coulomb balance of chemical valency, the electrons and atoms are achieved in the pure KTN crystal, which is disturbed when a K vacancy appears in the crystal. All atoms with positive valencies, such as K^{1+}, Ta^{5+}, and Nb^{5+}, will be closer to the vacancy due to the disappeared repulsion, whereas, the atoms with negative valance, O^{2-}, will be farther from the vacancy. Because of the stable structure of oxygen octahedron, the atomic displacements of Ta, Nb, and O atoms are at the same level. The relative small atomic displacements of K atoms are caused by the vacancy stemming from the relative further distances and weak Coulomb interaction between the K lattices. The reason for the variation in KTN with O vacancy is similar. With the Coulomb attraction of the other O atoms, the K, Ta and Nb atoms closed to the O vacancy will move away from the original position, and the other O atoms will move near the position of the defect. There are obvious differences in the atomic displacements of the KTN crystal with V_K^0 and V_O^0 defects compared with those vacancies V_K^{1-} and V_O^{2+}, respectively, which are caused by the charge compensation. Comparing V_O^0 with V_O^{2+}, as the influences of two doping electrons, the atomic displacements of K, O and Ta atoms in V_O^0 change less than that of V_O^{2+}. Comparing V_K^0 with V_K^{1-}, the atomic displacements of K, O and Ta atoms in V_K^0 change more than that of V_K^{1-}. The variation of atomic displacements could also be attributed to the Coulomb interaction after the charge compensation.

Electronic Properties of KTN with Different Vacancies

The total density of state (TDOS) and partial density of state (PDOS) of pure KTN are shown in Fig. 2a and b, respectively. The calculated band gap is 1.575 eV, which is consistent with the previous works.[11,35] However, it is smaller in comparison with the experimental value of $KTa_{0.65}Nb_{0.35}O_3$ with 3.6 eV,[36] and $KTa_{0.6}Nb_{0.4}O_3$ with 3.34 eV.[37] The reason for this difference is inadequate treatment of the charge inhomogeneity, dielectric screening and many-body effect.[38,39] From Fig. 2a, it can be found that the valence bands (VBs) of KTN could be mainly divided into two zones, one is the lower valence bands (−55 eV to −10 eV), the other is the upper valence bands (−6 eV to 0 eV). In the lower valence bands, there is no hybridization for the peaks of DOS, which are at the positions of −54 eV, −31 eV, −27 eV and −11 eV. The DOS peak of −16 eV comes from the hybridization among the O s orbitals, a part of Nb p and d orbitals and a part of Ta s and d orbitals. There are three peaks between −30 eV and −10 eV, and the positions and heights of DOS peaks are similar to previous investigation,[40] but are different from the results of the reference,[41] which is caused by different computational methods. The hybridization among O 2p, Nb 4d and Ta 5d orbitals constitute the upper valence bands. In addition, the conduction bands (CBs) are

Table II. Atomic displacements of K, Ta, Nb, and O atoms closest to the vacancy (fractional coordinate)

Atom	V_K^0	V_K^{1-}	V_O^0	V_O^{2+}
K	2.11×10^{-5}	1.001×10^{-7}	-0.73×10^{-2}	-1.32×10^{-2}
O	-4.21×10^{-3}	-4.18×10^{-3}	0.932×10^{-2}	2.76×10^{-2}
Ta	4.76×10^{-3}	3.53×10^{-3}	-1.52×10^{-2}	-1.63×10^{-2}
Nb	3.74×10^{-4}	4.68×10^{-4}	-1.30×10^{-2}	-0.892×10^{-2}

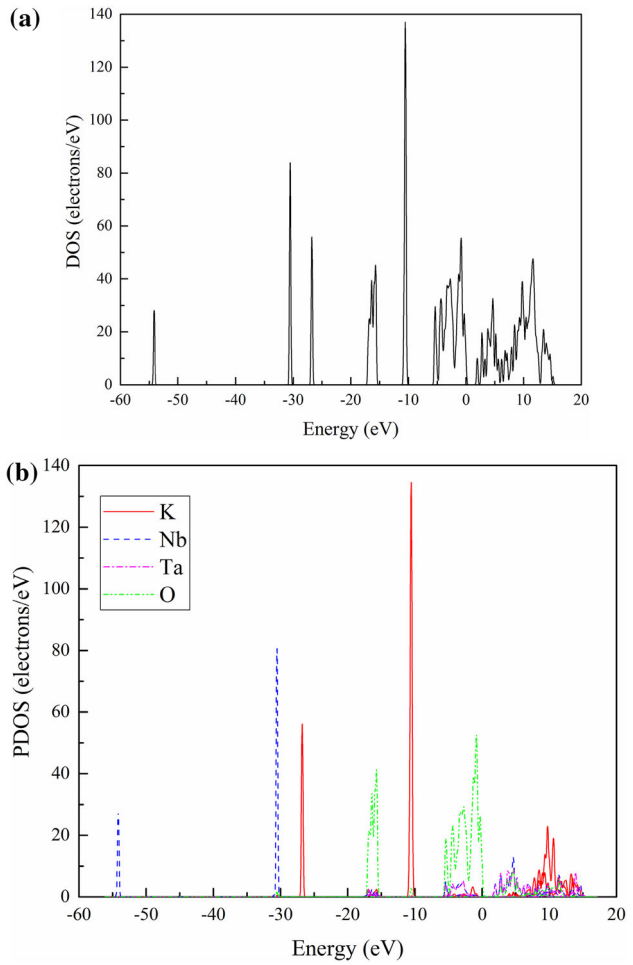

Fig. 2. Density of state of pure KTN. (a) The total density of state (TDOS), and (b) the partial density of state PDOS (K, O, Nb, Ta).

mainly composed of the Ta 5d and Nb 4d orbitals, and the contribution of O 2p is nearly zero at the conduction minimum, which is consistent with the results of references.[37,42]

Since the K vacancies caused by the high volatility of the K element are formed inevitably in the growth of the KTN crystal, ceramic and film, which is an important problem in the experiment, the density of state and band structure of K vacancies were indispensably studied. In order to investigate the impacts of electrons compensation on electronic structure, the density of state region (−8 eV to 6 eV) of the KTN with V_K^0 and V_K^{1-} were calculated, as shown in Fig. 3. As for V_K^0 and V_K^{1-}, the band gaps are 1.671 eV and 1.571 eV, respectively. Compared with the KTN crystal with V_K^{1-}, the conduction band of V_K^0 will move to the upper region, which causes the increase of band gap. It indicates that the compensation of electrons make the hybridization become stronger among Ta d, Nb d and O p orbitals. Besides, it is obvious that the band gaps of the KTN with neuter defect, V_K^0 (V_O^0), is larger than that with

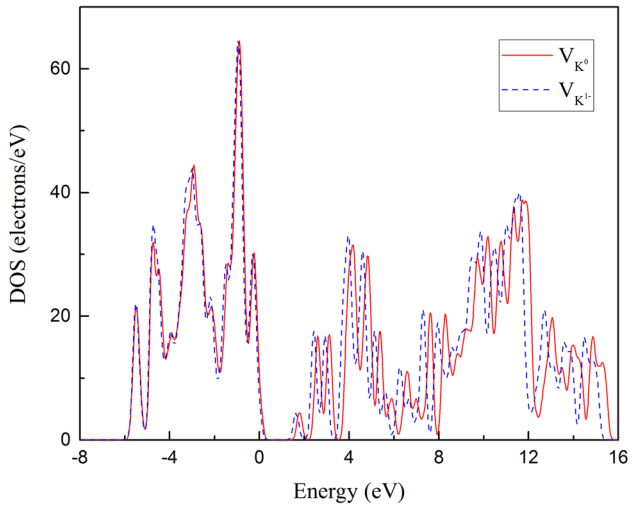

Fig. 3. Density of state region (−8 eV to 16 eV) of the KTN with V_K^0 and V_K^{1-}.

charged vacancies of V_K^{1-} (V_O^{2+}). This can be attributed to the hybridization interaction between the d orbital electrons of Ta, Nb atoms and the p orbital electrons of O atoms on the upper energy levels in neuter KTN crystal.

The Mulliken charge population of the Ta and Nb atoms is shown in Table III. In the KTN crystal with the V_O^0 and V_O^{2+}, the population of Ta and Nb atoms near the O vacancy are less than that of the other Ta and Nb. Compared with V_O^{2+}, the Mulliken population of Ta and Nb atoms in the KTN with V_O^0 both reduce after doping two electrons into the supercell, which may illustrate all the Ta^{5+} and Nb^{5+} ions are easier to attract the doped electrons. Besides, the variations of the interaction between Nb atoms and electrons are a little larger than that of Ta atoms and electrons, which indicates that the doped electrons have more significant influences on the Nb atoms than the Ta.

In the KTN crystal with V_K^0 and V_K^{1-} defects, the Mulliken populations are identical for the Ta atoms nearest to the vacancy and the other Ta atoms in the crystal. It indicates that the influences of the K vacancy on the Ta atoms at different positions are nearly the same, which is similar to the situation of Nb atoms in the crystal. Compared with V_K^{1-}, the Mulliken population of Ta and Nb atoms of the KTN with V_K^0 all increase, which indicates that the Mulliken population of all the Ta and Nb atoms are influenced by complement electrons. Besides, the population variation of the Nb is a little larger than that of Ta, which indicates that the charge compensation has more influence on the Nb atoms.

The Mulliken population and bond length of Ta-O and Nb-O bonds are listed in Table IV. Obviously, these parameters are changed when O vacancy or K vacancy appears. Compared with the pure KTN, the bond lengths of O-Nb and O-Ta of the KTN with V_O^{2+}

Table III. The Mulliken population of Ta, Nb atom

Parameter	$Ta_{nearest}$ (e)	Ta_{other} (e)	$Nb_{nearest}$ (e)	Nb_{other} (e)
Pure KTN	0.95	0.95	1.20	1.20
V_K^0	1.02	1.02	1.24	1.24
V_K^{1-}	0.95	0.95	1.15	1.15
V_O^0	0.62	0.92	0.89	1.16
V_O^{2+}	0.92	1.07	1.23	1.37

Table IV. The Mulliken population and the bond length of Ta-O and Nb-O bonds

Parameter	$Population_{Ta\text{-}O}$ (e)	$Length_{Ta\text{-}O}$ (Å)	$Population_{Nb\text{-}O}$ (e)	$Length_{Nb\text{-}O}$ (Å)
Pure KTN	0.71	2.02	0.57	1.970
V_K^0	0.70	2.003	0.55	1.964
V_K^{1-}	0.71	2.018	0.57	1.969
V_O^0	0.68	1.976	0.59	1.888
V_O^{2+}	0.78	1.905	0.56	1.845

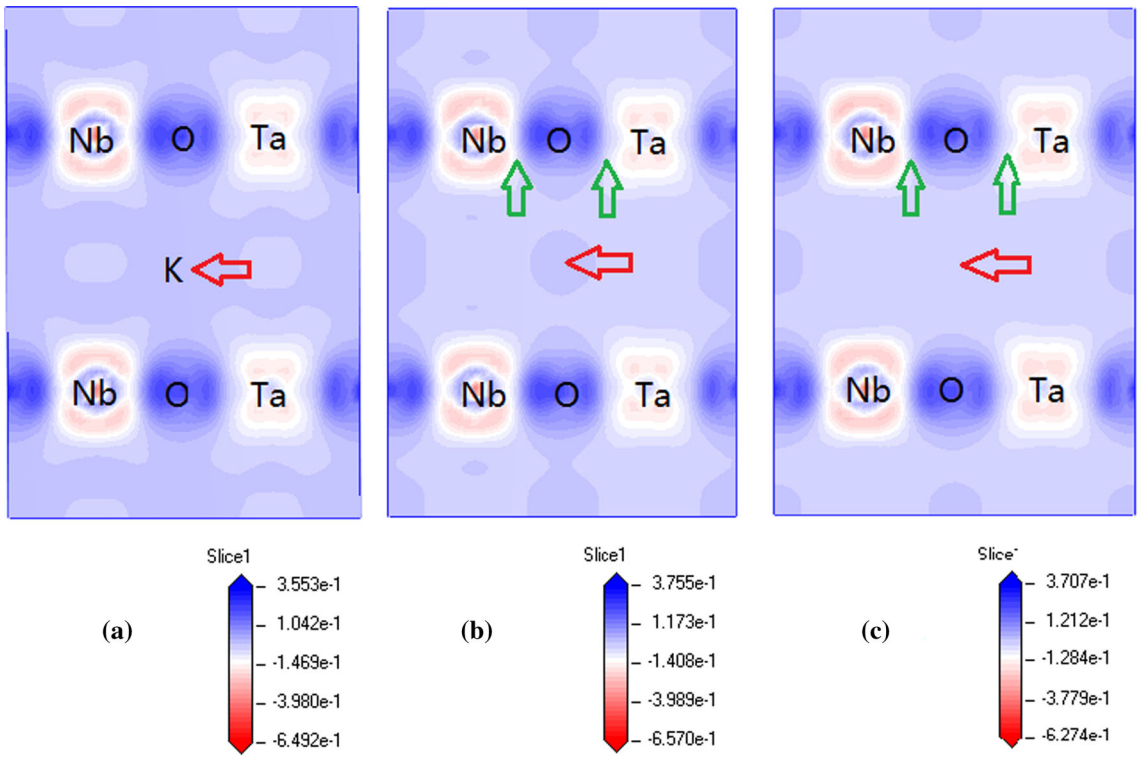

Fig. 4. Electron density difference of (a) pure KTN, (b) KTN with V_K^0, and (c) KTN with V_K^{1-}.

reduce by 0.125 Å and 0.115 Å, respectively, and the bond lengths of O-Nb and O-Ta of the KTN with V_O^0 reduce by 0.082 Å and 0.044 Å, respectively, which are caused by the lack of the intermediate O atom in the O-Nb-O-Ta-O. The Mulliken population of O-Nb and O-Ta vary from 0.56 e and 0.78 e to 0.59 e and 0.68 e, respectively. It illustrates that more electrons are obtained by O-Ta bond, which infers the interaction of O-Nb is stronger than that of the O-Ta bond.

Compared with pure KTN, the bond lengths of O-Nb and O-Ta in the KTN with V_K^0 reduce by 0.006 Å

and 0.017 Å, respectively, and the bond lengths of O-Nb and O-Ta of the KTN crystal with V_K^{1-} reduce by 0.001 Å and 0.002 Å, respectively. These variations indicate that the missing K atom has a greater effect on O-Ta bond and the interaction of O-Nb is stronger. In the crystal with V_K^0 defect, compared with the V_K^{1-} ones, the Mulliken population of O-Nb and O-Ta vary from 0.57 e and 0.71 e to 0.55 e and 0.70 e, respectively. It illustrates that more electrons are obtained by O-Ta bond and the interaction of O-Nb is stronger at the same time.

The differences of electron density of the pure KTN, KTN with V_K^0 and KTN with V_K^{1-} are shown in Fig. 4. It is obvious that the electron density between Nb and O is larger than Ta and O. It illustrates the interaction between Nb and O is stronger than the interaction between Ta and O, which is consistent with the results of atomic Milliken above. The electron distribution areas are marked by the inserted red arrow as shown in Fig. 4. The electron distribution area, around the missing K position in the KTN with V_K^{1-} in Fig. 4c, changes obviously. It can be seen in Fig. 4b that the electron distribution area between the position of missing K and oxygen octahedron of KTN with V_K^0 significantly reduces after the charge compensation. Besides, the electron clouds of positive ion will shrink in the position of the vacancy compared with the pure KTN. After the variation of the electron distribution, the electronic structure of KTN with V_K^0 is more stable than V_K^{1-} due to the chemical and Coulomb balance. It also can be confirmed by the variation of the lattice parameters. In addition, the electron densities of the Nb-O and Ta-O bond in the KTN with V_K^0 are larger than that of V_K^{1-}, which is marked by a blue arrow. It indicates that the interactions of the Nb-O and Ta-O bond are enhanced after the charge compensation in the crystal, and the electronic structure of KTN with V_K^0 becomes more stable compared with the KTN of V_K^{1-}.

CONCLUSIONS

In summary, the supercells of $KTa_{0.5}Nb_{0.5}O_3$ crystal with K and O vacancies, V_K^0, V_K^{1-}, V_O^0 and V_O^{2+} were established and optimized. The density functional simulation calculations have been used to investigate the effects of K and O vacancies on the structural and electronic properties. Significant changes have been found in the formation energy, atomic displacements, density of state, Mulliken population and chemical bonds, which are caused by the different vacancies in KTN. The band gaps of KTN with V_K^0, V_K^{1-}, V_O^0 and V_O^{2+} defects are 1.671 eV, 1.571 eV, 1.669 eV, and 1.577 eV, respectively. The formation energy of KTN with V_K^0 is lower than that of V_K^{1-}, and V_O^{2+} is lower than that of V_O^0, which means that the K vacancy with 0 charged, V_K^0, are likely to form in the KTN compared V_K^{1-}, with −1 charged K vacancy, and the O vacancy with +2 charge are easier to form in the KTN than V_O^0. Therefore, the KTN with different type of K and O vacancies present different formation ability, in addition, it is worth pointing out that charge compensation would obviously affect the stability of materials, which are conducive to analysis in experiments about the dielectric, mechanical and optical properties of KTN materials. The atomic displacements of Ta atoms in KTN with K and O vacancies are more easily influenced by the K and O vacancies than the Nb atoms. The compensation of electrons in KTN with vacancies caused stronger hybridization interaction among Ta d, Nb d and O p orbitals. And the complement electrons influenced Mulliken population of Ta and Nb atoms in KTN with charged vacancies, and the variation of the Mulliken population of Nb atoms is a little larger than that of Ta. In addition, the changes of Ta-O and Nb-O bond length, Mulliken population and electron density differences all illustrate that the interaction of the Nb-O bond is stronger. The distinct differences of the structure and properties with K and O vacancies are significant for the preparation and controlling of the KTN crystal and films.

ACKNOWLEDGEMENTS

This work was supported by the Natural Science Foundation of China (No. 11444004), the Natural Science Foundation of Heilongjiang Province (No. QC2015062) and the Natural Science Foundation of Heilongjiang Provincial Education Department (No. 12531115).

REFERENCES

1. D. Redfield, *Phys. Rev.* 130, 916 (1963).
2. M. Sirena, A. Zimmers, N. Haberkorn, E. Kaul, L.B. Steren, J. Lesueur, T. Wolf, Y.L. Gall, J.J. Grob, and G. J. Faini, *Appl. Phys.* 107, 113903 (2010).
3. Y. Amouyal, *Comput. Mater. Sci.* 78, 98 (2013).
4. S. Jantrasee, S. Pinitsoontorn, and P. Moontragoon, *J. Electron. Mater.* 43, 6 (2014).
5. J.W. Lee, H. Shichijo, H.L. Tsai, and R.J. Matyi, *Appl. Phys. Lett.* 50, 31 (1987).
6. I.N. Kholmanov, J. Edgeworth, E. Cavaliere, L. Gavioli, C. Magnuson, and R.S. Ruoff, *Adv. Mater.* 23, 1675 (2011).
7. D.C. Li, L. Fang, S.K. Deng, H.B. Ruan, M. Saleem, W.H. Wei, and C.Y. Kong, *J. Electron. Mater.* 40, 5 (2011).
8. E.A. Kotomin, R.I. Eglitis, and A.I. Popov, *J. Phys. Condens. Matter* 9, L315 (1997).
9. D.D. Cuong, B. Lee, K.M. Choi, H.S. Ahn, S. Han, and J. Lee, *Phys. Rev. Lett.* 98, 115503 (2007).
10. S. Körbel, P. Marton, and C. Elsässer, *Phys. Rev. B* 81, 174115 (2010).
11. Y. Shen and Z. Zhou, *Comput. Mater. Sci.* 65, 193 (2012).
12. R.I. Eglitis, *Int. J. Mod. Phys. B* 28, 1430009 (2014).
13. S.A. Prosandeyev, A.V. Fisenko, A.I. Riabchinski, I.A. Osipenko, I.P. Raevski, and N. Safontseva, *J. Phys. Condens. Matter* 8, 6705 (1996).
14. I.R. Shen and A.L. Ivanovskii, *Phys. Lett. A* 371, 155 (2007).
15. C.H. Park and D.J. Chadi, *Phys. Rev. B* 57, R13961 (1998).

16. A. Kushima, S. Yip, and B. Yildiz, *Phys. Rev. B* 82, 115435 (2010).
17. M. Choi, F. Oba, and I. Tanaka, *Phys. Rev. B* 78, 014115 (2008).
18. S.A. Prosandeyev and I.A. Osipenko, *Phys. Stat. Solidi B* 192, 37 (1995).
19. J.J. Zhang, G.Y. Gou, and B.C. Pan, *J. Phys. Chem. C* 118, 17254 (2014).
20. P. Günter and J.P. Huignard, *Photorefractive Effects and Materials, Photorefractive Materials and Their Applications I* (Berlin: Springer, 1988), pp. 7–73.
21. E. Cross, *Nature* 432, 24 (2004).
22. A. Rousseau, M. Guilloux-Viry, V. Bouquet, A. Perrin, G. Tanne, F. Huret, J.F. Seaux, D. Cros, and V. Madrangeas, *Ferroelectrics* 316, 7 (2005).
23. W. Yang, Z. Zhou, B. Yang, Y. Jiang, Y. Pei, H. Sun, and Y. Wang, *Appl. Surf. Sci.* 258, 3986 (2012).
24. M.D. Segall, P.J. Lindan, M.J. Probert, C.J. Pickard, P.J. Hasnip, S.J. Clark, and M.C. Payne, *J. Phys. Condens. Matter* 14, 2717 (2002).
25. D. Vanderbilt, *Phys. Rev. B* 41, 7892 (1990).
26. G. Sághi-Szabó and R.E. Cohen, *Ferroelectrics* 194, 287 (1997).
27. X. Wang, J. Wang, Y. Yu, H. Zhang, and R.I. Boughton, *J. Cryst. Growth* 293, 398 (2006).
28. Z. Zhang, P. Wu, L. Lu, and C. Shu, *Appl. Phys. Lett.* 88, 142902 (2006).
29. A.F. Kohan, G. Ceder, D. Morgan, and C.G. Van de Walle, *Phys. Rev. B* 61, 22 (2000).
30. L.X. Ning, W.P. Cheng, C.C. Zhou, C.K. Duan, and Y.F. Zhang, *J. Phys. Chem. C* 118, 19940 (2014).
31. C.B. Long, T.Y. Li, H.Q. Fan, Y. Wu, L.C. Zhou, Y.W. Li, L.H. Xiao, and Y.H. Li, *J. Alloys Compd.* 658, 839 (2016).
32. R. Sumang, C. Wicheanrat, T. Bonkkarn, and S. Maensiri, *Ceram. Int.* 3, 228 (2015).
33. L. Zhang, B.H. Sun, Q. Liu, N. Ding, H. Yang, L.X. Wang, and Q.T. Zhang, *J. Alloy. Compd.* 657, 27 (2016).
34. T.C. Yi, M. Lu, K. Yang, P.F. Xiao, and R. Wang, *Nucl. Instrum. Meth. Phys. Res. B* 335, 66 (2014).
35. Y. Shen, W. Wang, Z. Zhou, Y. Jiang, and C. Hou, *Comput. Mater. Sci.* 83, 294 (2014).
36. M. DiDomenico Jr and S.H. Wemple, *Phys. Rev.* 155, 539 (1967).
37. K. Zheng, D. Zhang, Z. Zhong, F. Yang, and X. Han, *Appl. Surf. Sci.* 256, 1317 (2009).
38. M.S. Hybertsen and S.G. Louie, *Phys. Rev. Lett.* 55, 13 (1985).
39. M.S. Hybertsen and S.G. Louie, *Phys. Rev. B* 34, 8 (1986).
40. Y. Shen and Z. Zhou, *J. Alloys Compd.* 466, 525 (2008).
41. Y.X. Wang, W.L. Zhong, C.L. Wang, and P.L. Zhang, *Phys. Lett. A* 285, 390 (2001).
42. D.J. Singh, *Phys. Rev. B* 53, 176 (1996).